ISSN: 2414-1895 DOI: 10.6919/ICJE.202407_10(7).0016

The Method of Ship Motion Attitude Forecasting based on NGO-VMD and Network Models

Qilong Wu, Lei Song*, Jiarui Huang, Cheng Wang, Xiaochen Jiang

Naval Architecture and Port Engineering College, Shandong Jiaotong University, Weihai 264209, China

Abstract

Due to the complex and dynamic nature of maritime environments, predicting vessel motion poses can provide precise decision support for vessel operations and timing, thus enhancing safety and efficiency at sea. In complex maritime environments, vessels may experience significant random fluctuations in motion. Relying on a single prediction model may lead to substantial prediction errors, thus impacting the accuracy of vessel motion prediction. Therefore, this paper proposes a method for predicting vessel motion poses based on the Northern Goshawk Optimization (NGO) algorithm, Variational Mode Decomposition (VMD), and Long Short-Term Memory (LSTM) neural networks. The proposed method utilizes NGO to search for the optimal parameters of VMD, which is then used to decompose vessel motion pose data into several modal components. Subsequently, each modal component is predicted using LSTM, and the predicted results are aggregated to obtain the final prediction. Experimental data from simulations of a bulk carrier vessel are used to validate the proposed method, comparing it with LSTM and VMD-LSTM models. The results demonstrate that the proposed method achieves higher prediction accuracy, offering a more efficient approach to vessel motion pose prediction.

Keywords

Ship; Motion Pose Prediction; Deep Learning; NGO; VMD; LSTM.

1. Introduction

In the presence of wind and waves at sea, ships typically undergo six degrees of freedom in motion: surge, sway, heave, roll, pitch, and yaw [1]. Different motions affect ship movement differently and continuously disrupt the normal operation of precision equipment on board, thereby reducing the safety and efficiency of maritime operations. To address these issues, a method for predicting future ship motion is proposed. Ship motion prediction involves forecasting future ship motion trends based on historical motion data, serving as a means to mitigate navigational risks. By predicting ship motion at future time instances, adjustments to the vessel can be made in advance to ensure the safety of maritime operations and the normal functioning of onboard equipment. Therefore, research on ship motion prediction holds significant practical significance [2].

In recent years, considerable attention has been devoted to predicting ship motion attitudes. Prediction methods primarily include statistical forecasting, convolution, grey prediction, Kalman filtering, time series analysis, neural networks, and ensemble forecasting [3]. Statistical forecasting, based on integral equation analysis, involves a highly complex computation process and is subject to numerous limitations, making its practical application in ship motion prediction challenging. Convolution [4] predicts ship motion under different sea conditions by analyzing the convolution of ship response functions and wave height measurement functions, yet its computational complexity and assumption of system linearity and invariance restrict its practical use. Grey prediction methods [5] are limited

ISSN: 2414-1895 DOI: 10.6919/ICJE.202407_10(7).0016

by the requirement of a moderate amount of training data and exhibit limitations in predicting nonlinear time series such as ship motion sequences. Kalman filtering theory [6] is relatively mature but is more suitable for linear systems, necessitating precise mathematical modeling of ship dynamics. Prediction accuracy significantly diminishes when oceanic environments undergo changes. Utilizing neural network methods and models involves training, learning, and adjusting network structures with historical data inputs [7]. However, the initial structural parameters of the network are often empirically set, leading to inadequate prediction accuracy in single neural network methods. Ensemble forecasting combines various methods to improve prediction accuracy by leveraging their respective strengths and integrating new models for further enhancement of predictive performance. Compared to single prediction methods, ensemble forecasting capitalizes on the predictions from multiple models to obtain more reliable results [8]-[9].

Due to the complexity and strong stochastic nature of current ship motion attitudes [10], single models encounter issues in practical applications, such as singular prediction results and inadequate prediction accuracy. Extensive experiments have demonstrated that compared to single models, ensemble prediction models exhibit higher accuracy and stability [11]. Therefore, this paper proposes a ship motion attitude forecasting method based on NGO-VMD-LSTM. Initially, the optimal parameters for VMD are determined through NGO search, followed by decomposing ship motion attitude data into several modal components using VMD. Subsequently, each modal component is predicted using LSTM, and the prediction results are aggregated to obtain the final prediction. Comparative experiments with LSTM and VMD-LSTM demonstrate that this method achieves the highest prediction accuracy, affirming its efficacy in ship motion attitude prediction.

2. Principle

2.1 Northern Goshawk Optimization

Based on the predatory behavior of the Northern Goshawk, Mohammad et al. proposed the Northern Goshawk Optimization (NGO) algorithm, primarily simulating the processes of identification and attack, pursuit and evasion that occur during predation [12].

(1) Identification and Attack Phase

During this phase, the Northern Goshawk searches the global space to randomly select prey and swiftly initiate attacks, aiming to enhance the algorithm's global exploration capability. The principle equation is as follows:

$$P_i = X_k, i = 1,2,..., N, k = 1,2,3..., i-1, i+1,..., N \tag{1}$$

$$X_{i,j}^{new,P1} = \begin{cases} x_{i,j} + r(P_{i,j} - I_{Xi,j}), F_{Pi} < F_i \\ x_{i,j} + r(X_{i,j} - P_{i,j}), F_{Pi} \geq F_i \end{cases} \tag{2}$$

$$X_i = \begin{cases} X_i^{new,P1}, F_i^{new,P1} < F_i \\ X_i, F_i^{new,P1} \geq F_i \end{cases} \tag{3}$$

In this equation, P_i represents the position of the i th Northern Goshawk; F_{P1} is the objective function value; k is a randomly selected integer within the range [1, N] excluding i; $X_{i,j}^{new,P1}$ denotes the new position of the i th Northern Goshawk in the first stage for dimension j; $X_i^{new,P1}$ is the updated position of th i -th Northern Goshawk; $F_i^{new,P1}$ is the objective function value of the i -th Northern Goshawk after the first stage update; r and I is a random number within the range [1, N].

ISSN: 2414-1895 DOI: 10.6919/ICJE.202407_10(7).0016

(2) Pursuit and Evasion Phase

During this phase, prey attempts to escape. Due to the Northern Goshawk's high-speed maneuverability, it can capture prey in almost any situation during the predation process. By simulating this action, the algorithm's utilization of local search in the global space is enhanced [13]. The principle equation is as follows:

$$x_{i,j}^{new,P2} = x_{i,j} + R(2r-1)x_{i,j} \tag{4}$$

$$R = 0.02(1-\frac{t}{T}) \tag{5}$$

$$Xi = \begin{cases} X_i^{new,P2}, F_i^{new,P2} < F_i \\ X_i, F_i^{new,P2} \geq F_i \end{cases} \tag{6}$$

In this equation, t represents the current iteration number and T denotes the maximum number of iterations; $X_i^{new,P2}$ is the updated position of the i-th Northern Goshawk; $X_{i,j}^{new,P2}$ is the new position of the i-th Northern Goshawk in the second stage; and $F_i^{new,P2}$ is the objective function value of the i-th Northern Goshawk after the update in the second stage.

2.2 Variational Mode Decomposition

Variational Mode Decomposition (VMD) serves as a time-frequency analysis method aimed at decomposing multi-component signals into several single-component amplitude-modulated signals. The VMD method overcomes common issues such as endpoint effects and mode mixing in the widely used Empirical Mode Decomposition (EMD) method by introducing variational optimization and regularization terms. It possesses a more robust mathematical theoretical foundation and is more suitable for handling nonlinear and non-stationary signals. The fundamental concept of VMD revolves around formulating and solving variational problems. It represents an adaptive, non-recursive sequence decomposition algorithm capable of adaptively decomposing an input sequence into k intrinsic mode functions (IMFs) based on the frequency domain characteristics of the signal [14]. The key stages of VMD include the following steps:

(1) Formulating the variational problem. To ensure the existence of a central frequency and a constrained bandwidth within each intrinsic mode function (IMF), a constraint condition is introduced. This condition aims to minimize the cumulative estimated bandwidth of all IMFs while requiring the summation of all IMFs to equal the original sequence. The corresponding mathematical expression is as follows:

$$\begin{gathered} \min_{\{uk\},\{\omega k\}} \sum_k \| \partial_t[(\delta(t)+\frac{j}{\pi t})u_k(t)]e^{-j\omega kt} \|_2^2 \\ s.t. \sum_k u_k = f \end{gathered} \tag{7}$$

In the equation, k denotes the number of iterations; u_k refers to the k-th component of the Variational Mode Decomposition (VMD); ω_k indicates the center frequency of the k-th mode component; $\delta(t)$ is the mutation function; and f represents the sequence of ship attitudes.

ISSN: 2414-1895 DOI: 10.6919/ICJE.202407_10(7).0016

(2) Transforming the constrained variational problem into an unconstrained one involves introducing a quadratic penalty factor represented by α and a Lagrange multiplier represented by λ. Thus, the augmented Lagrangian equation is obtained as follows:

$$\begin{aligned} Lu_k, w_k, \{\lambda\} = \alpha \sum_k \| \partial_t [(\delta(t) + \frac{j}{\pi t}) u_k(t)] e^{-j\omega kt} \|_2^2 + \\ \| f(t) - \sum_t u_k(t) \|_2^2 + \lambda(t), f(t) - \sum_k u_k(t) \end{aligned} \tag{8}$$

(3) Solving the unconstrained variational problem involves updating and iterating over $\{u\}$, $\{w\}$ and $\{\lambda\}$ using the alternating direction method of multipliers to locate the saddle point of Equation (7) and establish a cyclic process of updates. The corresponding mathematical expressions are as follows:

$$w_k^{n+1} = \frac{\int_0^\infty \left| \widehat{u_k}(w) \right|^2 dw}{\int_0^\infty |u_k(w)|^2 dw} \tag{10}$$

$$\lambda^{n+1}(w) \leftarrow \hat{\lambda}^n(w) + \tau \hat{f}(w) - \sum_{i=1}^n u_i^{n+1}(w) \tag{11}$$

$$\sum_k u_k^{n+1} - u_{k2}^{n2} / u_{k2}^{n2} < \varepsilon \tag{12}$$

Finally, we obtain:

$$\hat{u}_k^{n+1}(\omega) = \frac{\hat{f}(\omega) - \sum_{i \neq k} \hat{u}_i(\omega) + \frac{\hat{\lambda}(\omega)}{2}}{1 + 2\alpha(\omega - \omega_k)^2} \tag{13}$$

$$\omega_k^{n+1} = \frac{\int_0^\infty \omega \left| \hat{u}_k(\omega) \right|^2 \mathrm{d}\omega}{\int_0^\infty \left| \hat{u}_k(\omega) \right|^2 \mathrm{d}\omega} \tag{14}$$

2.3 NGO-Optimized VMD

The decomposition of signals using VMD requires appropriate parameter settings [K, α]. When the value of K is too large, over-decomposition may occur, whereas an undersized value may lead to under-decomposition. Similarly, if α is excessively large, there is a risk of losing frequency band information, whereas an undersized α may result in redundant information [15]. Hence, this paper employs the Northern Goshawk Optimization (NGO) algorithm to search for the optimal VMD parameters based on the characteristics and complexity of the signal variations. The flowchart of NGO-optimized VMD is illustrated in Fig. 1. Emulating the predatory behavior of the Northern Goshawk, the envelope entropy is employed as the fitness function to compute the fitness of each goshawk. The optimal objective function value is determined, and the corresponding optimal position is stored. Through iterative updates, the process continues until the stopping condition is met, yielding the optimal VMD parameters [K, α] via NGO optimization.

ISSN: 2414-1895 DOI: 10.6919/ICJE.202407_10(7).0016

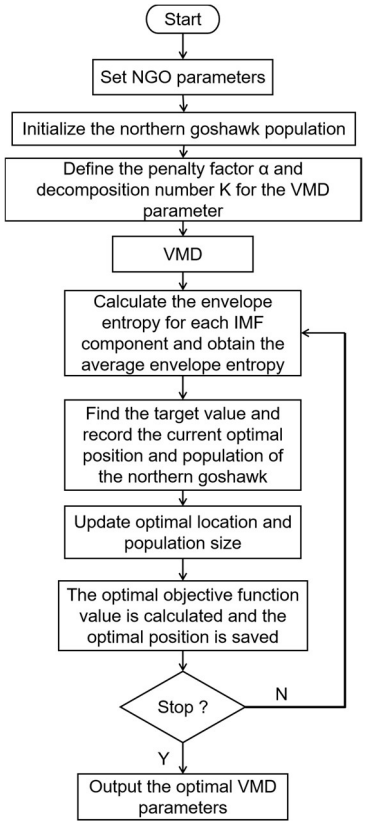

Fig. 1 NGO optimized VMD process diagram

2.4 Long Short-Term Memory Networks

Recurrent Neural Networks (RNNs) were introduced to directly incorporate time dependency into neural network structures. The core idea is to enhance the capabilities of typical artificial neural network methods by dynamically introducing sequential structures [16]. Although there are many techniques to achieve this functionality, Long Short-Term Memory (LSTM) networks have achieved remarkable success due to their ability to learn short-term and long-term dependencies in problems, and they are designed to address the vanishing gradient problem that plagues most recurrent neural network architectures. Additionally, because of its incorporation of both slow and fast phenomena, it is highly suitable for ship attitude prediction.

The primary information processing units in LSTM are called "cells." These cells can be seen as more complex neurons in typical Multilayer Perceptrons (MLPs). A unit comprises multiple gates to preserve and regulate the flow of information over arbitrary length sequences. This feature enables LSTM to determine which information is useful for long-term and short-term purposes, making it highly suitable for any type of sequence-based problem [17]. An LSTM unit can be defined as:

$$i_t = \sigma(W_{ii}x_t + b_{ii} + W_{hi}h_{t-1} + b_{hi}) \tag{15}$$

$$f_t = \sigma(W_{if}x_t + b_{if} + W_{hf}h_{t-1} + b_{hf}) \tag{16}$$

$$g_t = tanh(W_{ig}x_t + b_{ig} + W_{hg}h_{t-1} + b_{hg}) \tag{17}$$

$$o_t = \sigma(W_{io}x_t + b_{io} + W_{ho}h_{t-1} + b_{ho}) \tag{18}$$

ISSN: 2414-1895 DOI: 10.6919/ICJE.202407_10(7).0016

$$c_t = f \odot c_{t-1} + i_t \odot g_t \tag{19}$$

$$h_t = o_t \odot tanh(c_t) \tag{20}$$

In the equation, x and h represent the input and hidden states, respectively, at the current time step t . $\odot$ denotes the element-wise multiplication operation (Hadamard Product), and σ represents the Sigmoid activation function. f_t, i_t, and o_t denote the forget, input, and output gates, respectively, at the current state. W_{xy} and b_{xy} represent the learnable weights and bias terms between x and y gates . For a clear understanding of the flow of information within the LSTM unit, refer to the schematic diagram in Fig. 2.

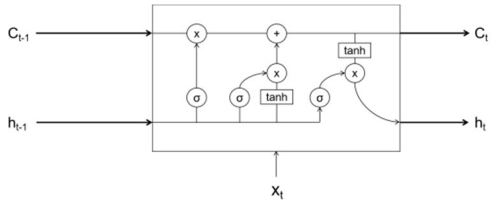

Fig. 2 LSTM cell

Similar to neurons, LSTM units can be interconnected to transmit temporal information and can be stacked like layers.

3. NGO-VMD-LSTM Prediction Method

Due to the complex and variable maritime environment, ship motion is influenced by various factors, making it challenging for a single model to accurately predict ship motion attitudes [18]. Therefore, a prediction method based on NGO-VMD-LSTM is proposed.

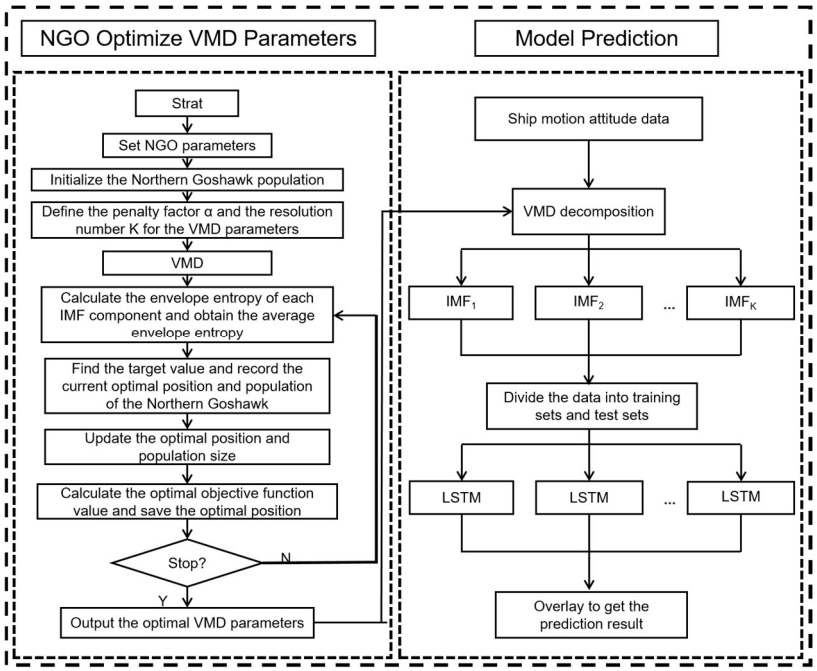

Fig. 3 NGO-VMD-LSTM Ship Motion Attitude Prediction Method Flowchart

ISSN: 2414-1895 DOI: 10.6919/ICJE.202407_10(7).0016

First, the NGO parameters are set, and the Northern Goshawk Optimization algorithm is initialized. The VMD penalty factor α and the number of decompositions k are defined as the parameters to be optimized. These parameters are used to decompose the ship motion attitude data, resulting in modal components such as IMF1, IMF2, ..., IMFk. Next, an LSTM model is constructed for the prediction of each modal component individually. Finally, the prediction results of each modal component are aggregated to obtain the final prediction. The process is illustrated in Fig. 3.

4. Prediction based on Ship Motion Attitude Data

This study uses roll, pitch, and heave displacement data obtained from simulations of a bulk carrier model in Unreal Engine 5.3. Each type of data consists of 3000 sets, with a sampling interval of 0.1 seconds. The ship has an overall length of 225 meters, a beam of 32.3 meters, a depth of 18 meters, and a draft of 13 meters. The ship model is depicted in Fig. 4. The experimental environment includes Windows 11 (64-bit), a 2.3 GHz CPU (Intel i7-12700H), an NVIDIA GeForce RTX 3060 GPU, and 16 GB of memory. PyCharm was used as the development tool, Python as the programming language, PyTorch as the deep learning framework, and Unreal Engine 5.3.

Fig. 4 a bulk carrier model

4.1 NGO-VMD Decomposition

Taking pitch as an example, the scatter plot of the data is shown in Fig. 5. Since the data used is obtained through simulation, no data preprocessing is required, and it can be used directly. The parameters for the Northern Goshawk Optimization algorithm are as follows: the population size is set to 20, the dimensionality is set to 2, the lower limits for the penalty factor α and the number of decompositions k are [100, 3], the upper limits are [2500, 9], and the maximum number of iterations is 40. The decomposition results are shown in Fig. 6.

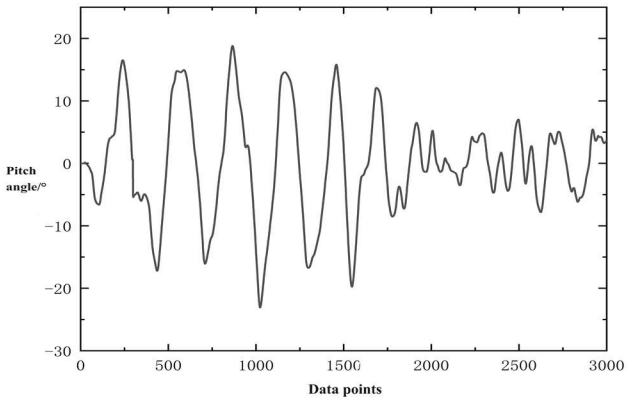

Fig. 5 Scatter plot of pitch angle data

ISSN: 2414-1895 DOI: 10.6919/ICJE.202407_10(7).0016

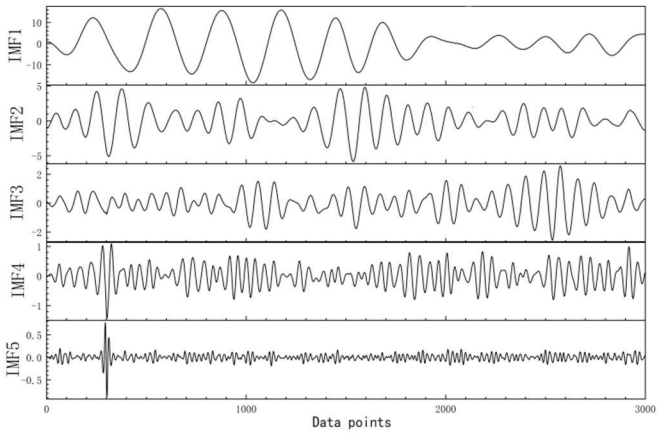

Fig. 6 Decomposition results

4.2 Results and Analysis

In this paper, the Mean Absolute Error (MAE), Mean Absolute Percentage Error (MAPE), and Root Mean Square Error (RMSE) are used as evaluation metrics for the prediction accuracy of the model. The formulas for these metrics are as follows:

$$MAE(X,h)=\frac{1}{m}\sum_{i=1}^{m}|h(x_i)-y_i| \tag{21}$$

$$MAPE=\frac{1}{n}\sum_{i=1}^{n}|\frac{\hat{x}(i)-x(i)}{x(i)}|\times 100\% \tag{22}$$

$$RMSE=\sqrt{\frac{\sum_{j=1}^{n}(x_j-\hat{x}_j)^2}{n}} \tag{23}$$

To more clearly demonstrate the accuracy of the NGO-VMD-LSTM model in predicting ship motion attitudes, predictions were also conducted using the LSTM model and the VMD-LSTM model. Based on the simulated data, the ratio of the training set to the test set was set to 8:2. The hidden layer size was set to 128, the number of layers to 2, the dropout rate to 0.2, the learning rate to 0.001, the number of training epochs to 50, and the batch size to 128. The trends in the loss function and the prediction results are shown in Figs 7-10.

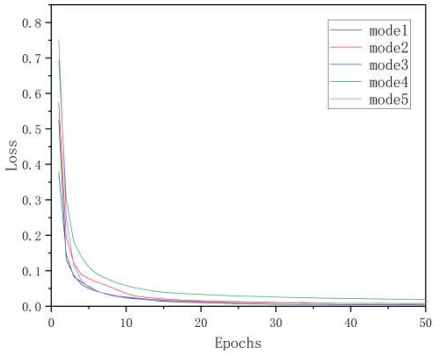

Fig. 7 Model loss function curve

ISSN: 2414-1895 DOI: 10.6919/ICJE.202407_10(7).0016

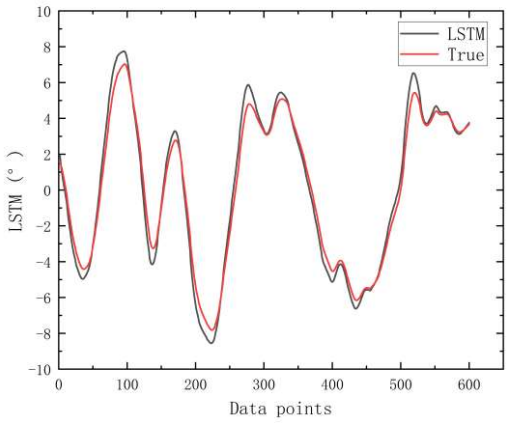

Fig. 8 LSTM model prediction results

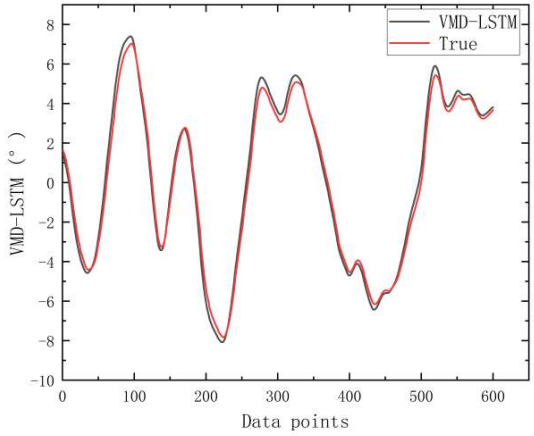

Fig. 9 VMD-LSTM model prediction results

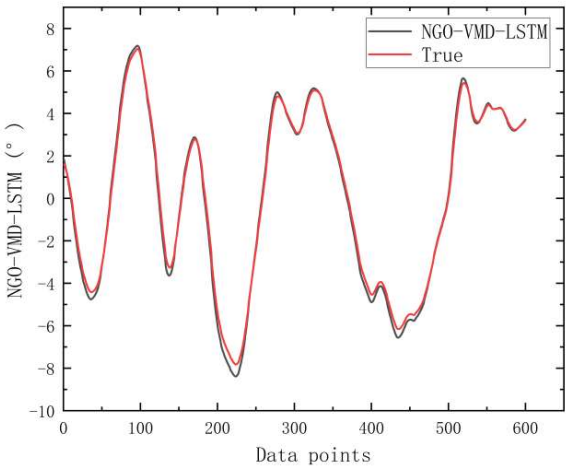

Fig. 10 NGO-VMD-LSTM model prediction results

ISSN: 2414-1895 DOI: 10.6919/ICJE.202407_10(7).0016

Table 1. error statistics table

Error / Model	MAE	MAPE	RMSE
LSTM	0.5078	48.6431	0.6143
VMD-LSTM	0.3757	38.5773	0.4372
NGO-VMD-LSTM	0.2193	19.0656	0.2699

By analyzing Figs 7-10 and Table 1, it can be observed that with the increase in training epochs, the training loss decreases rapidly at the beginning and then stabilizes after a sharp decline, indicating that the model has converged. The prediction results of the three models generally follow the same trend as the actual values. However, the NGO-VMD-LSTM model shows a closer fit to the actual values compared to the LSTM and VMD-LSTM models. Specifically, the Mean Absolute Error (MAE) is reduced by 0.2885 and 0.1564, the Mean Absolute Percentage Error (MAPE) is reduced by 29.5757 and 19.5117, and the Root Mean Square Error (RMSE) is reduced by 0.3444 and 0.1673, respectively. This demonstrates that the combination of NGO and VMD can effectively enhance the performance of the LSTM network in predicting ship motion attitudes. The MAE, MAPE, and RMSE of the NGO-VMD-LSTM model are all lower than those of the LSTM and VMD-LSTM models, indicating that the NGO-VMD-LSTM model provides better prediction accuracy for ship motion attitude.

5. Conclusion

Due to the randomness and complexity of the maritime environment, this paper proposes a ship motion attitude prediction method based on NGO-VMD-LSTM. This model optimizes VMD using NGO, then decomposes the ship motion attitude data into several modal components using the optimized VMD. Each modal component is predicted using LSTM, and the final prediction is obtained by aggregating the predictions of all modal components. Comparative experiments with the LSTM and VMD-LSTM models show that the proposed method reduces various evaluation metrics and produces predictions that are closer to the actual values. This provides a new approach for predicting ship motion attitudes.

References

[1] Zheng, Q. (2019). Design of a six-degree-of-freedom simulation system in ship simulators. Ship Science and Technology, 41(04), 34-36.

[2] Yuan, Q. M., Wang, S. Z., Han, B., et al. (2022). Analysis method of ship motion attitude under wave forecast uncertainty. China Navigation, 45(01), 31-36.

[3] Zuo, S. Y., Zhao, Q., Zhang, B., et al. (2022). Ship motion attitude prediction based on VMD-SSA-GRU. Ship Science and Technology, 44(23), 60-65+69.

[4] Kaplan, P. (1969). A study of prediction techniques for aircraft carrier motions at sea. Hydronautics, 3(3), 121-131.

[5] Zhang, X. B., Liu, B. H., Yu, K. B., et al. (2020). Research on variable length empirical mode decomposition method based on gray prediction. Advances in Marine Science, 38(03), 493-503.

[6] Qiao, S. J., Han, N., Zhu, X. W., et al. (2018). Dynamic trajectory prediction algorithm based on Kalman filter. Journal of Electronics, 46(02), 418-423.

[7] Yumori, I. (1981). Real-time prediction of ship response to ocean waves using time series analysis. In Oceans. IEEE.

[8] Yang, G., Jie, Q. M., & Tao, N. Q. (2017). Prediction of ship motion attitude based on BP network. In 2017 29th Chinese Control and Decision Conference (CCDC).

[9] Guo-Dong, W., Bin, H., & Wen-Yun, S. (2017). Short-term prediction of ship motion based on LSTM. Ship Science and Technology.

ISSN: 2414-1895 DOI: 10.6919/ICJE.202407_10(7).0016

[10] Peng, B. Z. H. (2019). An improved particle swarm optimization algorithm applied to long short-term memory neural network for ship motion attitude prediction. Transactions of the Institute of Measurement and Control, 41(15).

[11] Zhang, B., Peng, X. Y., & Gao, J. (2020). Ship motion attitude prediction based on ELM-EMD-LSTM combined model. Ship Mechanics, 24(11), 1413-1421.

[12] Liu, Y. G. (2023). Fault diagnosis and prediction model for pumped storage water pump based on NGO-SSA optimized SVM algorithm. Guangxi Electric Power, 46(03), 8-14.

[13] Li, C. Y., & Zheng, D. J. (2023). NGO-XGBoost dam deformation prediction model based on multi-level data processing and its application. Hydropower Energy Science, 41(11), 77-81.

[14] Wei, H. X., Cheng, H., Wu, W., et al. (2024). Rolling bearing fault diagnosis based on VMD visualization and deep learning. Journal of Mechanical Design and Manufacturing, 1-6 [2024-03-29].

[15] Xu, W. S., Zhang, L., & Wang, H. (2024). Prediction of Kuroshio temperature front intensity in the East China Sea based on edge extraction and VMD-LSTM. Advances in Marine Science, 1-12 [2024-03-30].

[16] Lian, Q. Y., Sun, W., & Li, R. S. (2024). Short-term ship traffic flow prediction model based on attention mechanism and stacked LSTM. Journal of Dalian Maritime University, 1-10 [2024-03-29].

[17] Han, X., Sun, W. B., Zhou, Z. N., et al. (2023). Prediction of ship navigation position based on LSTM neural network. Ship Electronic Engineering, 43(09), 58-61.

[18] Yan, X. P., Liu, J. L., Zhang, Y., et al. (2022). Research status and prospects of intelligent shipping. Modern Transportation and Metallurgical Materials, 2(01), 7-18.